Energy and Built Environment xxx (xxxx) xxx

Contents lists available at ScienceDirect

Energy and Built Environment

journal homepage: http://www.keaipublishing.com/en/journals/energy-and-built-environment/

Full Length Article

Submicron-sized airborne pathogen trajectory simulations for infection control in a large hospital ward ☆

Kwun Hei Cheung, Tsz Wun Tsang, Kwok Wai Mui, Ling Tim Wong*

Department of Building Environment and Energy Engineering, The Hong Kong Polytechnic University, Hong Kong 999077, China

ARTICLE INFO

Keywords:
Hospital ward
Ventilation
Airborne pathogen
Infection control

ABSTRACT

Understanding the spatial distribution of viral-sized airborne pathogens helps determine infection control strategies to reduce cross-infection risks in hospital ward-shared environments. Through Computational Fluid Dynamics (CFD) simulations of pathogen transmission trajectories with a user-defined bioaerosol drag, this study evaluates the effectiveness of localized ventilation systems and physical barriers in limiting submicron-sized pathogen dispersion within a corridor-linked hospital ward. In particular, sneezing episodes by an infected patient at 24 bed positions in a general inpatient ward with four semi-open cubicles, a nursing station, a washroom and two storage rooms accessible by a common corridor were evaluated numerically. The results showed that only 20% of the released airborne contaminants went into the corridor, with a suspension time of over five minutes. Their movement paths were strongly influenced by exhaust units from adjacent cubicles. Using a privacy curtain was more effective than localized ventilation in reducing particle dispersion, and using both strategies together further improved the reduction performance. These findings emphasize the necessity of considering submicron-sized airborne pathogen in infection risk estimation and inform key design criteria for an effective ventilation system to reduce infection risks in large hospital wards.

1. Introduction

Pandemics pose significant challenges to healthcare systems and harm societal health [1,2]. In recent years, particularly following the COVID-19 pandemic, attention has been focused on airborne transmission, as it plays a crucial role in spreading respiratory infectious diseases through the release of respiratory droplets from coughing, sneezing, and talking [3]. An infectious patient in a healthcare facility can lead to pathogen contamination in the surrounding air [4], causing superspreading events that contribute to nosocomial outbreaks [5,6]. The movement and travel distance of these droplets vary by their sizes [7,8], with submicron-sized droplets remaining suspended in the air for an extended period, facilitating long-range airborne transmission and increasing the infection risk through inhalation by the recipient [9,10]. However, these sizes are often overlooked in the literature due to either the complexity of the investigation or a lack of evidence suggesting their prevalence in common respiratory events. The long-range transmission of contaminated aerosols in large shared environments remains under investigation [11].

Building ventilation has been recognized as an effective strategy for mitigating airborne infection risks. Air distribution aims to deliver fresh air to all areas while effectively diluting and eventually expelling pollutants. An efficient building ventilation system is characterized by sufficient ventilation rate, proper airflow direction, and air distribution [12]. In addition to a centralized ventilation system for general usage, targeted ventilation, such as personalized ventilation (PV), is implemented to facilitate local air distribution by positioning ventilation units near the occupant [13]. The performance of PV systems has been evaluated in various healthcare settings and has proven effective in minimizing spatial distribution within inpatient cubicles [14–18].

Privacy curtains around patient beds acted as physical barriers to reduce local air exchange efficiency in the breathing zone, which could help prevent cross-infection [19–21]. Further research studies are needed to investigate the effectiveness of physical barriers on local air distribution in specific indoor environments [22,23].

Given the severity of historical and recent nosocomial outbreaks, research focus on evaluating and reducing cross-infection risk within ward environments has become prominent.

The pathogen transmission patterns in the wards housing six patients across different ventilation scenarios were studied using Computational Fluid Dynamics (CFD) [24]. Long-range airborne transmission is a concern in typical large shared inpatient wards accessed by medical facilities and function rooms from a common corridor [25,26]. A few studies have examined cross-infection risks in corridor areas [27,28]. However,

☆ Peer review under the responsibility of Southwest Jiaotong University.

* Corresponding author.
E-mail address: ling-tim.wong@polyu.edu.hk (L.T. Wong).

https://doi.org/10.1016/j.enbenv.2025.08.004
Received 19 May 2025; Received in revised form 18 August 2025; Accepted 25 August 2025
Available online xxx

Table 1
Summary of case settings.

	Case 1	Case 2	Case 3	Case 4
Description				
Simulated Scenario	Sneezing episode by a bed-lying, infected inpatient			
Number of scenarios	24 in all bed locations			
Discrete Particle	Droplet nuclei of MERS-CoV virus			
Cubicle ACH	9			
Local Air Exhausts	0% (Off)		30% of cubicle supply air	
Patient Privacy Curtain	Open	Closed	Open	Closed
Supply Air Flow Rate Settings (m/s)				
S1, S3, S4, S6, S7, S9, S10, S12 (0.6 × 0.6m)	0		1.105	
S2, S5, S8, S11 (0.6 × 0.6m)	3.315		1.105	
S13 (0.6 × 0.6m)	0.530			
Air Exhaust Ratio Setting (per exhaust unit)				
E1, E2 (0.3 × 0.3m)	0.0690		0.0490	
E3, E4, E5, E6 (0.35 × 0.6m)	0.126		0.0900	
E7 (0.3 × 0.6m)	0.265		0.189	
E8 (0.3 × 0.6m)	0.0912		0.0650	
24 Local Air Exhausts (0.2 × 0.2m)	0		0.0120	

most studies adopted gas concentration to predict airborne transmission, neglecting the behavioral nature of aerosol movement that includes deposition and diffusion mechanisms. Studies on discrete particles have focused on sizes over 1 μm, where the drag force is the dominant factor influencing aerosol movement instead of diffusion, which plays a more significant role in the behavior of submicron particles.

The study aims to understand how localized ventilation and physical barriers in shared ward settings alter local airflow and reduce airborne infection risks originating from inpatient cubicles with multiple potential aerosol emission sources. An experimentally validated drag constant is adopted in the CFD simulations for the movement of submicron-size particles, surpassing the limitations of accuracy inherent in the default particle drag model [29]. Extended end-to-end pathogen transport replicating long-range transmission trends is numerically examined to provide references for determining effective strategies to control nosocomial transmission.

2. Materials and methods

2.1. Inpatient ward & transmitted pathogen deposition

This study adopts a physical hospital inpatient ward in operation as the study location. Notably, a nosocomial outbreak occurred in this ward during the SARS outbreak in Hong Kong in 2003. The ward is a typical inpatient ward measuring 24.5 m (L) × 18 m (W) × 2.7 m (H), with two inpatient cubicles on each side, along with a nursing station, a washroom, and two storage rooms, all accessible via a common corridor, as presented in Fig. 1. Each cubicle has six beds with bedside cabinets. Surrounding the beds are curtains hung from overhead tracks that can be closed for privacy, with air gaps of 0.7 m at the top and 0.15 m at the bottom. Ventilation is supplied by ceiling-mounted air supply diffusers located within the cubicle, while air exhausts are located on the ceiling of the common corridor and in the washroom at the end of the corridor, ideally providing an airflow pathway from clean zones to dirty zones.

The effects of ventilation arrangements and physical barriers on air distribution are evaluated. The ventilation rate of 9 air changes per hour (ACH) was maintained in all simulated cases. The air change rate and air exhaust ratios of the exhaust vents E1–E8 were obtained from a field study to ensure a realistic ventilation environment [30]. More details on the ventilation configurations can be found in Table 1. Four scenarios were simulated: Case 1 serves as the baseline scenario for comparison, with the original ventilation arrangement and configuration of the actual ward; Case 2 implements patient privacy curtains as physical barriers; Case 3 introduces three ceiling supply diffusers and local exhausts positioned behind the bed; and Case 4 combines both localized ventilation and the privacy curtains. Since pathogen release from respiratory processes is arbitrary, 24 sneezing episodes from all 24 beds were simulated to evaluate the average spatial effectiveness of contaminant removal by implementing infection control strategies.

Simulation results were analyzed and discussed using two approaches. First, particle deposition was evaluated to quantify the relative infection risk to occupants based on the accumulation of particles on surfaces in the ward. The Mann-Whitney U test was used to determine the statistical significance of the deposition data, with a p-value set as the significance level $\alpha = 0.01$. Second, particle trajectories were examined to provide a qualitative perspective on the movement and behavior of airborne particles during their suspension process in the air for long-range transmission.

2.2. Numerical simulations

This study used the finite-volume-based CFD code Ansys Fluent 13.0 to solve airflow as a continuum phase in the Eulerian framework. Airborne particle transport was considered a discrete phase in the Lagrangian framework [31]. For turbulent airflow prediction, the Reynolds-averaged Navier-Stokes (RANS) equations provide a decomposed form of flow quantities for calculating time-averaged and Reynolds stress components. The complexity of simulating turbulent flow is reduced by applying the RANS equations [32]. In the RANS framework, the renormalization group (RNG) *k*-epsilon model was used to predict indoor air distribution [33]. The governing equations were discretized using second-order upwind schemes, and pressure-velocity coupling was done using the SIMPLE algorithm. The Boussinesq approximation model predicted the mild buoyancy-driven flow indoors [34].

Table 2 lists the details for the boundary condition settings. To satisfy the mass balance condition within the domain, the amount of air sup-

Table 2
Boundary conditions in Ansys Fluent.

Entity	Boundary Conditions
S1–S13	Boundary type: Velocity Inlet Air temperature: 285K Direction: 15 degrees from the ceiling DPM type: Reflect
E1–E8, local exhausts	Boundary type: Outflow DPM type: Escape
Ceiling, floor, walls, beds, cabinets, washroom facilities	Boundary Type: Wall Heat flux: None DPM type: Trap
Inpatient bodies	Type: Wall Heat flux: 23.3W/m^2 DPM type: Trap (body), reflect (mouth)

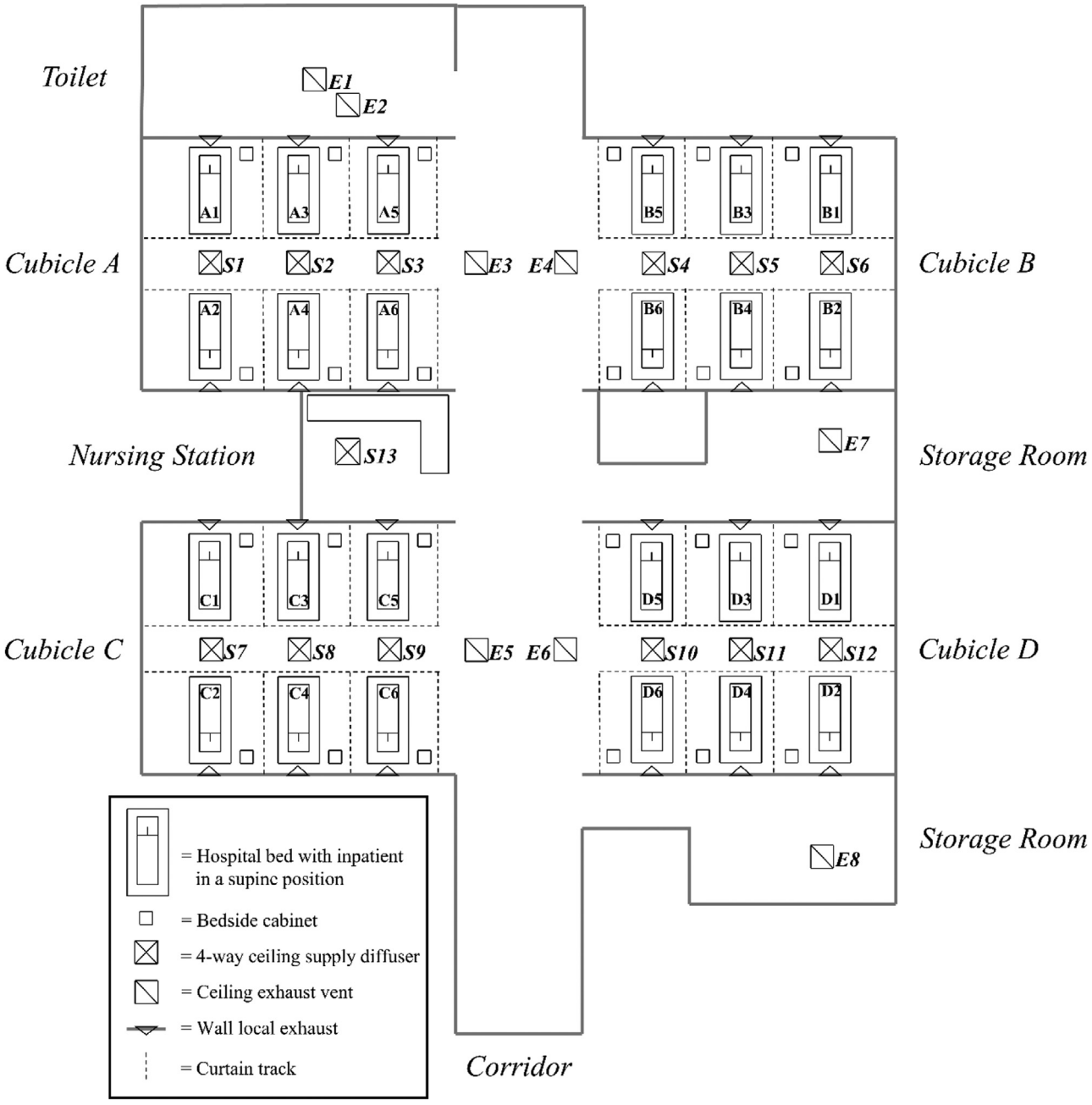

Fig. 1. A general inpatient ward [30].

plied had to equal the amount of exhausted air. The inpatient body was modelled as the heat source of the domain, with half of the heat transferred through convection, equivalent to 23.3W/m^2 convective heat being emitted from the body surface [35].

Particle trajectories are primarily influenced by the airflow field generated by internal ventilation, with minimal temperature difference between the internal wall surfaces, floor, and ceiling. In this hospital ward layout, the external walls are located on the inner side of the cubicles, contrary to the direction of particle transport towards the exhaust areas. As a result, the residence time for particles near the external walls is very short, with limited influence. Consequently, all concrete walls, ceiling, and floor were set as adiabatic. External heat sources, such as solar radiation, lighting, and equipment, were not considered in this study.

The airborne particle transport was modelled using the discrete phase modeling (DPM) function in Ansys Fluent. The particle motion equation used to predict discrete particle movement is expressed in Eq. (1):

$$\frac{du_b}{dt} = \frac{18\mu}{\rho_b d_b^2}\frac{C_D Re}{24}\left(u_a - u_b\right) + \frac{g_a\left(\rho_b - \rho_a\right)}{\rho_b} + F_x \tag{1}$$

where subscript a and b refer to the parameters for air and particle, μ is the molecular viscosity of air, ρ is the density, d is the diameter, C_D is the drag coefficient, Re is the particle Reynolds number, and F_x is the auxiliary forces acting on the particles. C_D and Re are expressed in Eqs. (2) and (3):

$$C_D = K_D/Re;\ Re < 1 \tag{2}$$

$$Re = \frac{\left(u_a - u_b\right)d_b\rho_a}{\mu} \tag{3}$$

where K_D is the bioaerosol drag constant and is expressed in Eq. (4):

$$K_D = d_b^2/2 \quad (4)$$

The validity of Eqs. (2) and (4) for bioaerosol diameters ranging from 0.69 μm to 6.9 μm have been proven previously, and it has been demonstrated that particles as small as 0.054 μm also fit well with these equations [29].

The properties of the coronavirus (MERS-CoV), with the aerodynamic diameter of the viral droplet nuclei at 0.167±0.012 μm and the bioaerosol density at 1,100 kg·m^{-3} are referenced. The Discrete Random Walk (DRW) model included velocity fluctuation for turbulent motion [36]. Several assumptions were made for the particle injection modelling [37]:

1) The heat and mass transfer between the air-particle and the particle-particle, where interactions were neglected.
2) Particles deposited on surfaces were immediately renounced (trap condition).
3) Particle coagulation was neglected for deposition.
4) All particles were modelled as spherical with the same particle size.
5) Only Brownian, thermophoretic, and Saffman lift forces were considered.

Other driving forces, which are insignificant to the particle trajectory (such as basset, magus and virtual mass force), were considered insignificant [38]. In the initial phase of a sneeze, expelled droplets undergo rapid evaporation within a short period (<0.1s) [7]. The droplet's size and internal state reach a more stable condition after this period, irrespective of whether complete liquid vaporization occurs, which exerts a limited influence on its subsequent trajectory. While the primary focus of this study is the long-range dispersion of viral droplet nuclei, the evaporation effect was neglected for simplicity. Likewise, for small-sized particles with diameters less than 10 μm, their trajectory is predominantly driven by the local airflow. The influence of the initial exhalation jet attenuates beyond a short distance [39,40]. Thus, the transient exhalation jet created by the sneeze was disregarded in a steady-state flow field. A total of 10,000 particles were simultaneously injected upward from the mouth of an infected individual in the supine position to simulate a sneezing event. This sample size was determined from a sensitivity analysis, which suggested that the variation in deposition was less than 1% between particles 20,000 and 100,000.

2.3. Grid independence study

An unstructured tetrahedral mesh was developed using the Ansys Workbench. Four grid cases with different grid sizes were generated for the grid independence study, with the controllable global element size set as 0.3 m, 0.18 m, 0.15 m, and 0.1 m. The size of the near-wall meshes is kept below 80% of that of the free-stream meshes to maintain the necessary resolution. One hundred air velocity data points were measured at the vertical line at the cubicle center (Line 1) and the horizontal line beside the diffuser air jet (Line 2). The velocity profiles are shown in Fig. 2. Considering the sequential relative error calculation based on the previous case with a smaller mesh size, the relative error for the mesh cases of 4.6 million, 6.1 million and 11 million cells are 10.28%, 18.26%, and 4.24% for Line 1, and 11.2%, 0.09%, and 3.2% for Line 2, respectively. The mesh case with 11 million cells, which exhibited a consistent flow field and smaller relative error, was therefore chosen for this study. Adopting the enhanced wall treatment model, the y-plus values for the inpatient's bodies were below 8, while most other ward surfaces remained below 15 to ensure adequate mesh refinement and accommodate the large surface areas in the domain [41].

2.4. Numerical validation

The measured ventilation airflow field with a heated human body was used for numerical validation [42]. Fig. 3a demonstrates a strong resemblance between the velocity profiles from the measurement data and the simulation results. The current simulation settings were deemed suitable for further examination of the flow field. The particle modelling was also validated previously [18]. Fig. 3b suggests that the simulation result aligns reasonably well with the deposition pattern reported in the literature. The DPM settings are considered valid and were adopted for further analysis.

3. Results and discussion

3.1. Cubicle airflow distribution

The fresh air distribution under different ventilation arrangements is shown in Fig. 4. In environments with minimal thermal gradients, the supply diffuser is characterized by directing air horizontally along the ceiling toward the walls for effective diffusion. Case 1 is the baseline scenario with the original ventilation arrangement in which a single supply diffuser directs two air jets toward beds 3 and 4, creating localized airflow in these positions. In contrast, beds 1, 2, 5, and 6 do not receive directed fresh air. Case 2 showed that the privacy curtain isolated these beds from the fresh air inflow, resulting in an imbalance in airflow distribution within the cubicle space. Additional supply diffusers in Case 3 distribute fresh air evenly, directing jets toward all bed positions.

As demonstrated in Fig. 5, the localized exhaust units near the beds in Case 3 established a new pathway for contaminant removal. This arrangement allows sneezing particles to be drawn to the exhaust and nearby surfaces rather than dispersing along the inpatient thermal plume to other areas. In Case 4, the privacy curtain creates distinct air zones by dividing the inpatient spaces, working with localized ventilation to promote uniform air circulation within each inpatient area. In this case, the simulated air jet profile resembles the streamline of a four-way supply diffuser implemented in a private single hospital room [43].

3.2. Particle deposition distribution

The particle deposition results from the four simulation cases are given in Tables A1–A4. in the appendix. Across all settings, 32% to 82% of the particles deposited on the infector shortly after release. Deposition on other inpatients in the same cubicle was recorded at the highest rate at 3.5% (Case 1, Bed B3). Most particles exited their originating cubicle and deposited in the corridor, with the highest rate recorded at 16% (Case 1, Bed C5). Other areas had minimal deposition, the highest being 3.4% (Case 3, Bed A5) in the washroom and 5.1% (Case 3, Bed A6) in the nursing station. The affected areas were closest to the emission sources in these two cases, less than 20% of particles escaped from the originating cubicle in all scenarios. Less than 10% of particles escaped in 90% of simulation scenarios, indicating limited dispersion to other areas. This observation is consistent with a study of high cubicle concentration from a tracer gas simulation in a hospital ward [44].

The privacy curtain and local ventilation worked well in reducing particle dispersion: the privacy curtain in Case 2 captured between 7.7% and 28.3% of the particles, while the local exhausts in Case 3 captured between 0.4% and 12.1%. In Case 4, where both were utilized, the particle deposition ranged from 6.6% to 18.6%. Notably, privacy curtains capture airborne particles passively through mechanisms such as diffusion, interception, or inertial forces, while localized ventilation captures these particles by establishing an airflow pattern that directs airflow towards the exhausts. These two capturing methods may conflict with each other, so that once the airflow pattern changes, the number of suspended particles that could potentially collide with the privacy curtain may vary. The increase in deposition from implementing both strategies is not additive. Thus, this case shall be evaluated separately.

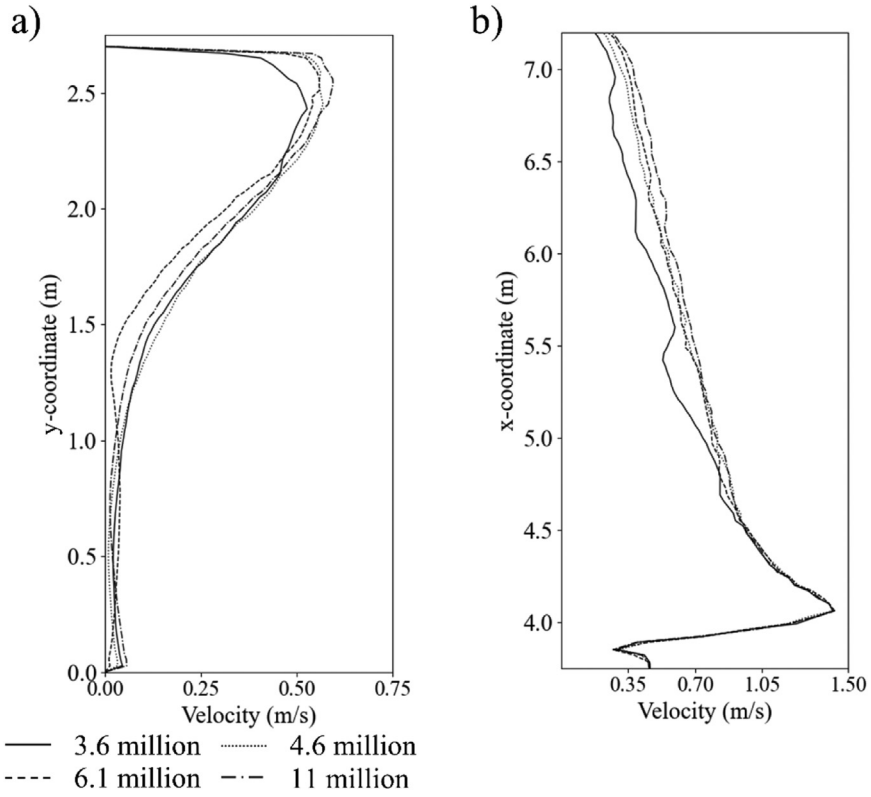

Fig. 2. Velocity plot of a) Line 1 and b) Line 2 for grid independence study.

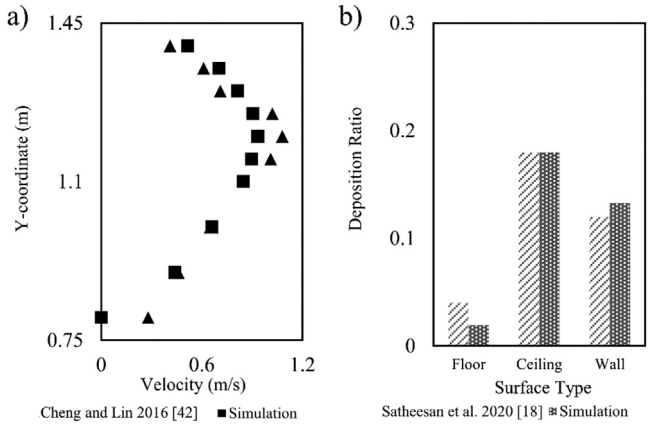

Fig. 3. Validation result for the case of a) airflow field and b) particle modelling [18,42].

The Discrete Random Walk (DRW) model and Brownian motion both account for the stochastic movement of submicron particles. The randomness from the DRW model is driven by the turbulent kinetic energy originating from turbulent eddies in the airflow field. However, the airflow field in the cubicle and corridor is predominantly calm and of low velocity, with fresh air actively diffused into the ambient air within the top cubicle region. The airflow under the room air condition is not favorable for generating significant random motion via the DRW model.

Instead, the observed particle random motion is primarily attributable to Brownian motion, which becomes more pronounced for particles of submicron or nanoscale size. The resulting high deposition rate to the infector could be attributed to this random movement, as it enhances collision frequency among the high concentration of particles near the body during the initial sneeze phase. As a result, there is a lower escape ratio from the cubicle (<20%) for subsequent particle dispersion, contrasting with the behavior of larger particles (>1μm) typically examined in mainstream literature.

3.3. Influence of ventilation arrangement on particle deposition

Table 3 summarizes the deposition data for case comparison. With Case 1 as the baseline, the deposition on inpatients from the same cubicle decreased from 1.3% to 0.4% in Case 2 with the privacy curtain and was nearly negligible in Case 4 when both arrangements were utilized. Case 3 showed a 0.6% reduction with localized ventilation, but this reduction was statistically insignificant. A similar result was observed in corridor deposition, which reduced from 3.8% to 1.6% in Case 2 and 1.0% in Case 4, with no significant change in Case 3. Case 4 had the lowest deposition in the cubicles and the corridor, indicating a potential benefit of using privacy curtains and localized exhaust to mitigate short- and long-range transmission. Meanwhile, changes in deposition were minor in the washroom and nursing station. The significant distance between these rooms and emission sources suggests that the cubicle arrangements had a diminishing influence over distance on particle dispersion for long-range transmission.

3.4. Spatial heterogeneity for sneezing sources

Spatial heterogeneity is evident across different sneezing locations. Table 4 compares the depositions based on source locations. Variations in deposition on other inpatients were observed with inconsistent trends, indicating that a single airflow pattern did not dominate the particle movement within the cubicle. Ventilation arrangements significantly influenced the local airflow pattern. Sneezing closer to the cubicle exit increases the chance of particles traveling to the corridor, facilitating long-range transmission.

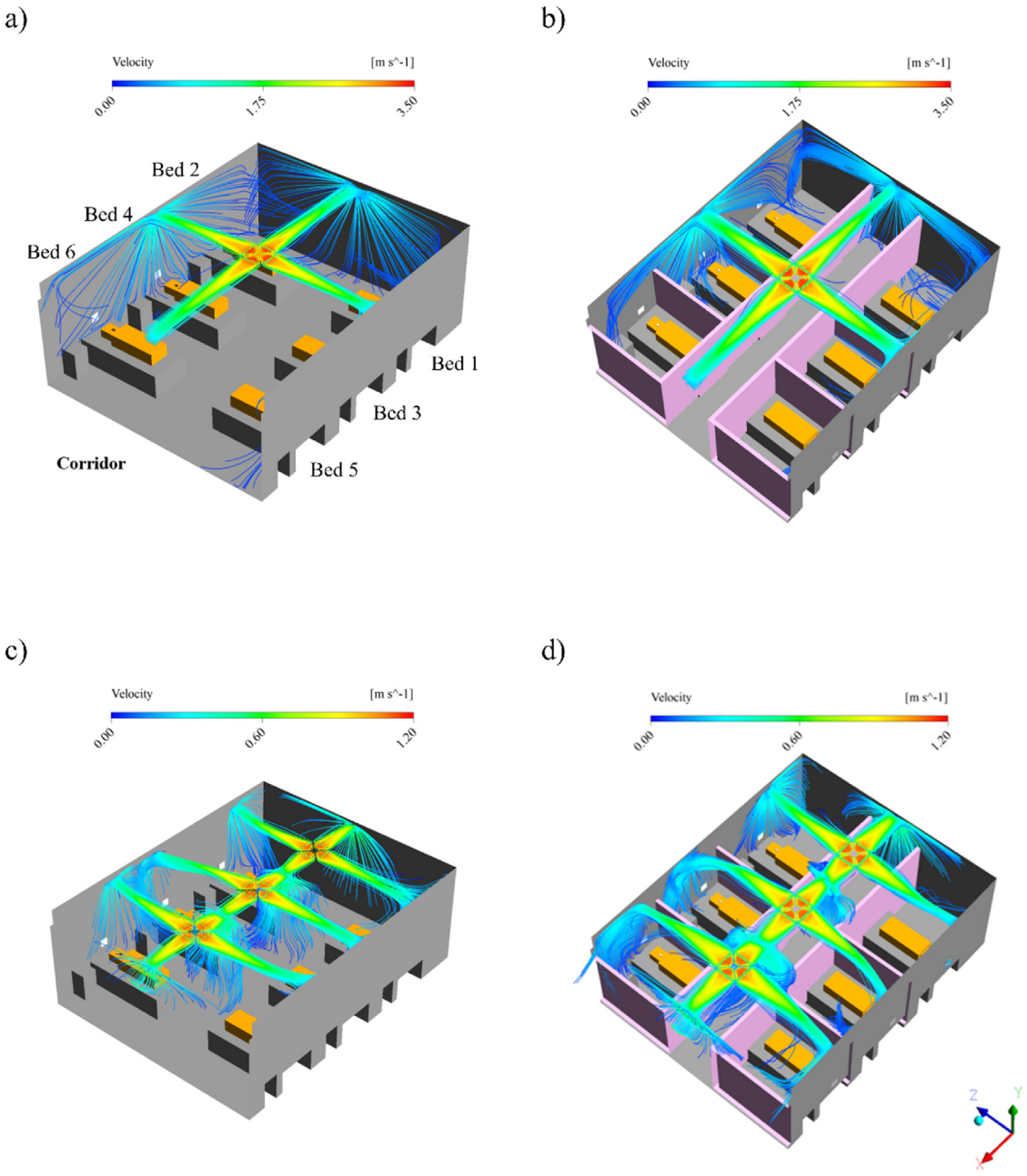

Fig. 4. Simulated cubicle air jet in a) Case 1, b) Case 2, c) Case 3, and d) Case 4.

Table 3
Comparison by case.

	Case 1 (Baseline)	Case 2		Case 3		Case 4	
Surfaces	Mean	Mean	p[a]	Mean	p	Mean	p
Infector	59.7%	54.5%	0.205	53.6%	0.013	58.4%	0.781
Inpatients from the same cubicle	1.3%	0.4%	<0.01	0.7%	0.081	0.0%	<0.01
Corridor	3.8%	1.6%	<0.01	3.5%	0.781	1.0%	<0.01
Washroom[b]	0.33%	0.16%	0.088	0.63%	0.624	0.09%	0.040
Nursing Station	0.09%	0.05%	0.015	0.34%	0.468	0.05%	0.024

[a] p-value with significance level $\alpha = 0.01$
[b] Emissions from Cubicles C and D were excluded due to absence of deposition

Table 4
Comparison by bed position.

	Beds 1,2 (Baseline)	Beds 3,4		Beds 5,6	
	Mean	Mean	p[a]	Mean	p
Inpatients from the same cubicle					
Case 1	0.8%	2.6%	<0.01	0.4%	0.130
Case 2	0.8%	0.2%	<0.01	0.1%	<0.01
Case 3	0.7%	0.9%	0.441	0.4%	0.105
Case 4	0.03%	0.02%	0.462	0.07%	0.021
Corridor					
Case 1	1.8%	1.2%	0.645	8.5%	<0.01
Case 2	0.9%	0.6%	<0.01	3.2%	<0.01
Case 3	0.7%	3.7%	<0.01	6.2%	<0.01
Case 4	0.4%	0.3%	0.4	2.3%	<0.01

[a] p-value with significance level $\alpha = 0.01$

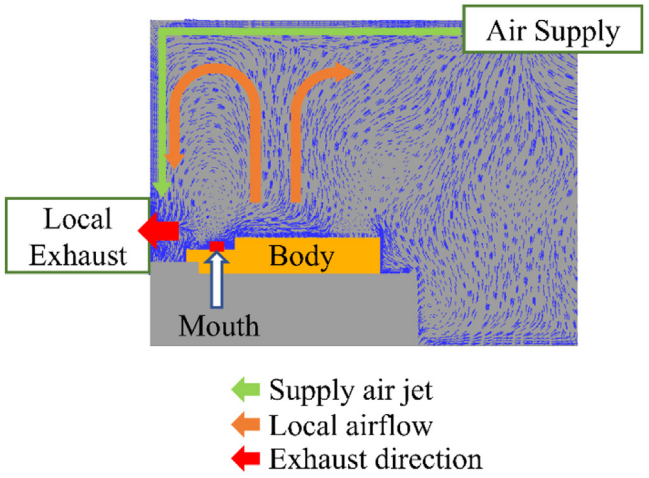

Fig. 5. Local airflow around inpatient in Case 3.

Notably, when sneezing occurred at the center (i.e., bed 3 and bed 4) of the cubicle, the deposition on inpatients from the same cubicle was the highest in Case 1. The corridor deposition was statistically lower in Case 2. These results could be attributed to the beds' alignment with the centrally located supply air jet in Cases 1 and 2.

3.5. Influence of ventilation arrangement on particle suspension

The impact of ventilation arrangements on particle suspension is evaluated by the trajectory coverage shown in Fig. 6.

The trajectory paths showed that the Case 1 supply configuration may recirculate contaminants and promote transmission. Particularly for beds 1 and 2, some suspended particles were caught in the supply air jet, causing them to escape into the corridor and potentially move into the opposite cubicle.

Case 3 demonstrated the effectiveness of localized ventilation in mitigating the penetration of external contaminants through balanced airflow distribution. The number of particles infiltrating the opposite cubicle was markedly reduced. However, some escaped particles took time to settle and remained suspended in the air for over 5 min (indicated by the red color in the graph), increasing airborne exposure risk in the corridor.

Cases 2 and 4 exhibited that the implementation of the privacy curtain prevented particles from moving across the cubicle. Suspension in the cubicle and corridor was reduced, resulting in a decreased infection risk for inpatients opposite the sneezing individual. The presence of a curtain significantly influences airflow distribution by obstructing local air propagation [19]. While the differences in trajectory trends between Cases 2 and 4 remain inconclusive, the overall impact of localized ventilation on altering particle movement was minimal from a macro perspective.

3.6. Particle suspension for long-range transmission

The particle trajectories shown in Fig. 6 indicate the particle suspension behavior contributing to long-range transmission. The particles must traverse the corridor before reaching other areas. In all cases, most suspended particles remained within the cubicle during the first minute after a sneeze. The suspension times recorded in Table 5 show that 1% of the particles remained suspended for over 5 min for bed positions near the corridor (Bed 5 and 6), which is more likely to travel to adjacent zones outside the cubicle. The particle movement within the corridor was irregular, as it navigated without a defined path or destination. In Cases 1 and 3, where long-range transmission is more pronounced, particles from a sneeze are often segregated and drawn toward exhausts in different rooms. The complex movement paths in the corridor resulted in an extended particle suspension, increasing the infection risk to occupants passing through the corridor.

3.7. Practical implications

While a localized ventilation strategy was found effective for suspended particle removal in inpatient cubicles [45], this study showed that it is challenging to depend solely on localized ventilation for airflow control in extended, large, and shared spaces. Installing a privacy curtain is a convenient measure during emergencies to enhance infection control without modifying the existing mechanical ventilation settings. New ventilation plan using localized ventilation strategy for retrofitting wards should integrate privacy curtains or other forms of inpatient partition as part of the ventilation configuration, which is essential to maximize the effectiveness of units aimed at suppressing particle dispersion.

The results indicated that a low proportion of particles escaped the cubicle. Airborne transmission of viral-sized pathogens across multiple zones is unlikely, but it can remain suspended in the air for a considerable amount of time that creates exposure risk to occupants. The airflow from exhausts in adjacent cubicles had minimal impact on the corridor's local airflow and caused low ventilation efficiency for contaminant removal. Corridor ventilation should be enhanced to reduce the occupant's exposure to airborne contaminants. Incorporating corridor air supply units or increasing exhaust capacity could reduce the infection risk by directing airborne particles toward designated areas for effective contamination removal.

Spatial heterogeneity provides critical insights into inpatient positioning. For sneezing, the dispersion of particles to adjacent zones, which occurs away from the corridor, could be minimized. Inpatients

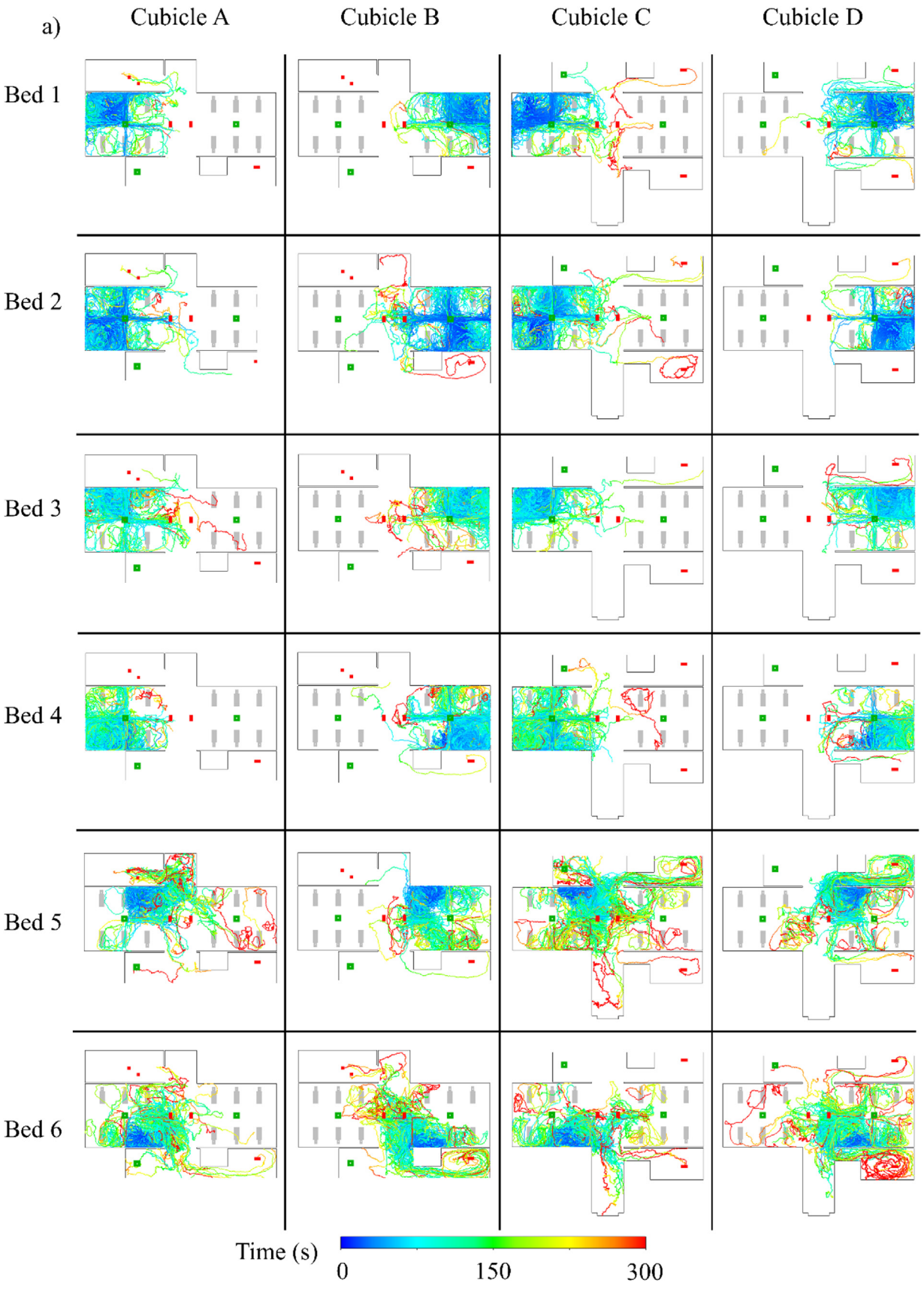

Fig. 6. Particle trajectory in a) Case 1, b) Case 2, c) Case 3, and d) Case 4.

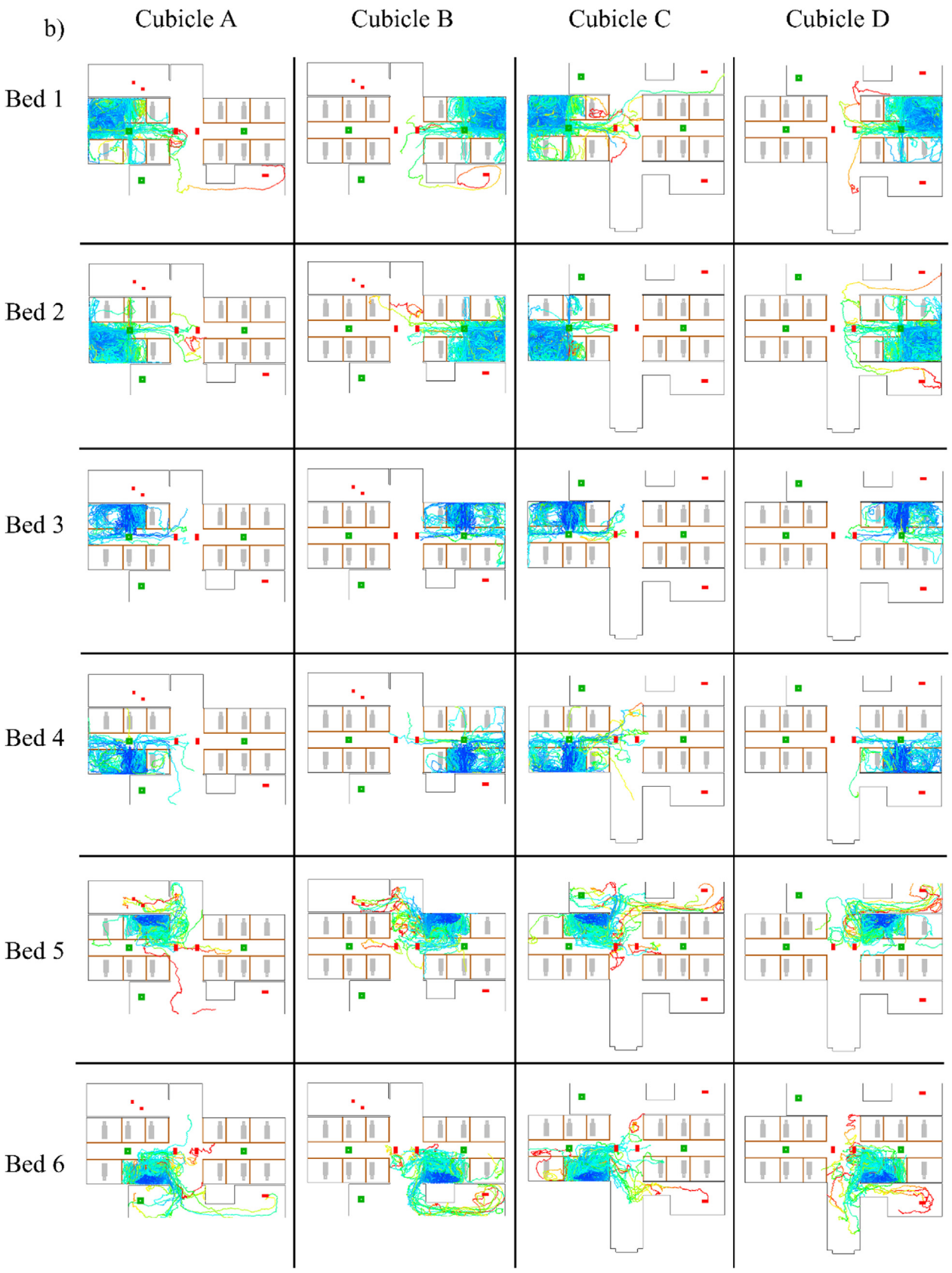

Fig. 6. Continued

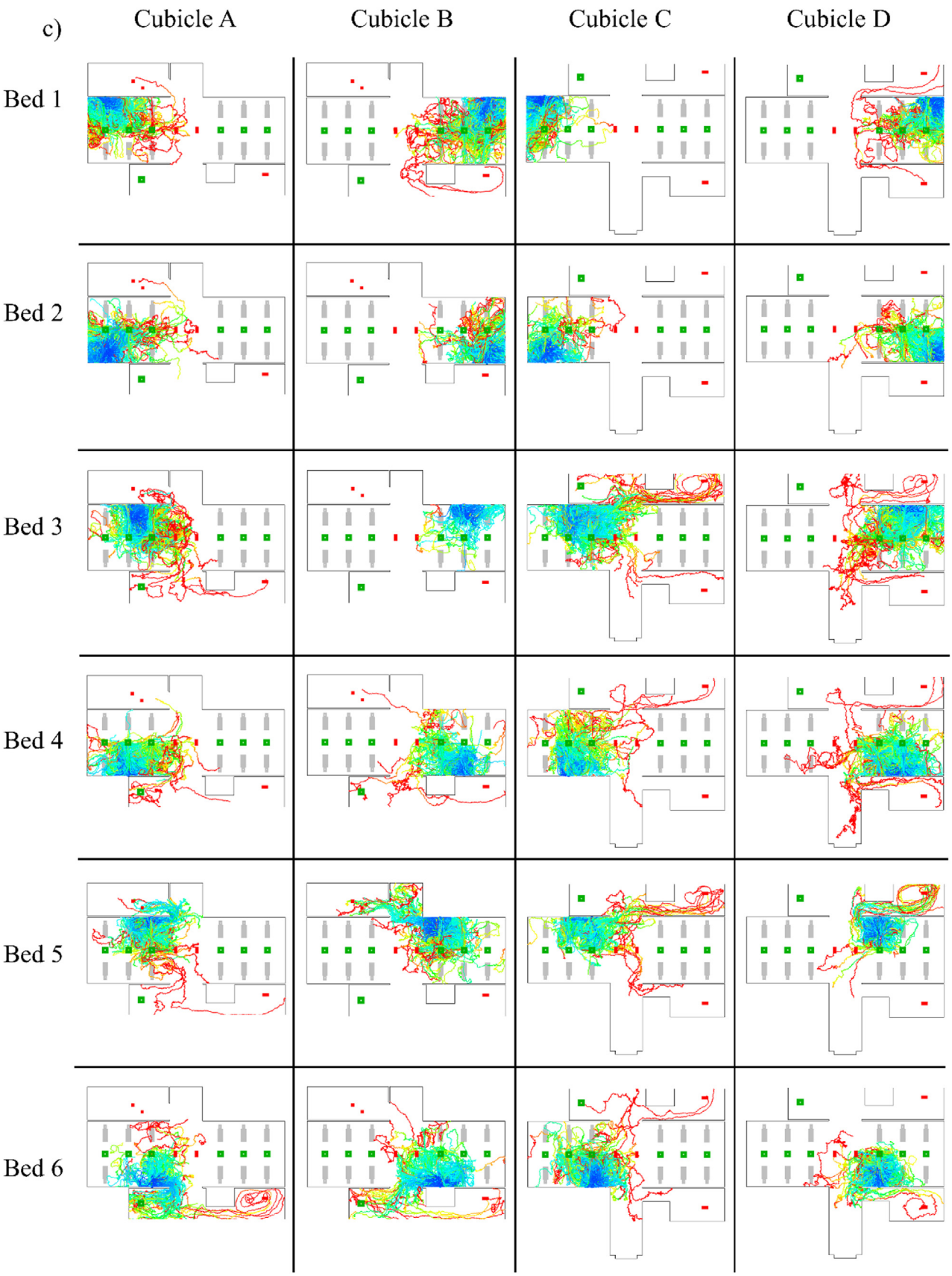

Fig. 6. Continued

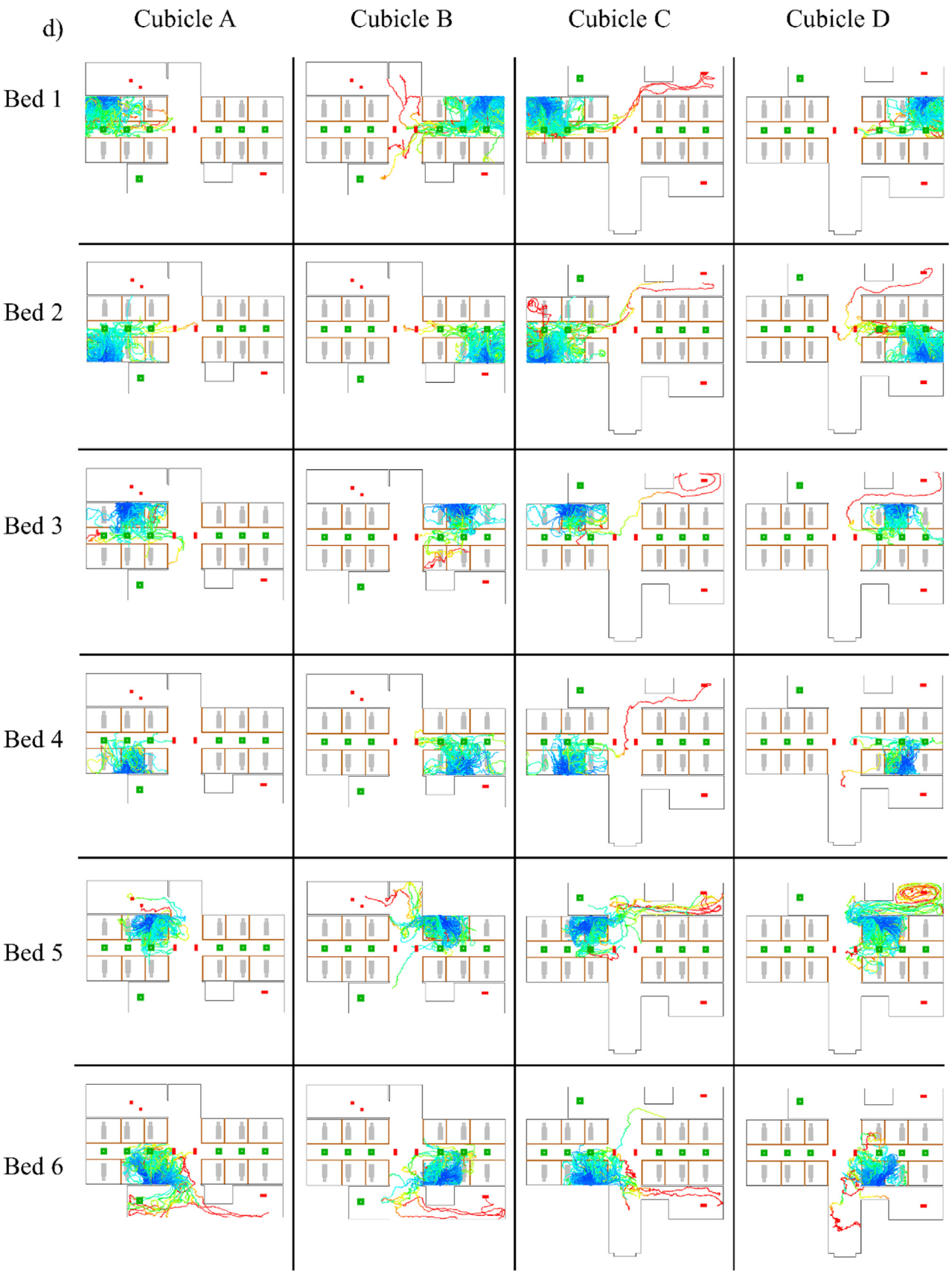

Fig. 6. Continued

Table 5
Suspension times for Cubicle A in Case 1.

Suspension time	Bed A1	Bed A2	Bed A3	Bed A4	Bed A5	Bed A6
>30 s	35.3%	31.8%	35.7%	37.4%	28.8%	28.0%
>1 min	13.9%	15.5%	22.6%	22.3%	18.5%	17.0%
>2 min	5.0%	5.6%	6.2%	6.8%	9.0%	10.8%
>3 min	2.1%	2.5%	2.6%	2.5%	4.3%	5.3%
>4 min	1.3%	1.3%	1.0%	0.5%	3.1%	2.7%
>5 min	0.3%	0.6%	0.3%	0.3%	1.6%	1.3%

exhibiting severe respiratory symptoms could be placed in beds away from the corridor.

Patients susceptible to different diseases may increase the risk of cross-infection in the same cubicle. Strategic patient isolation based on disease status mitigates this risk.

4. Conclusion

This study evaluated indoor ventilation strategies in a corridor-linked inpatient ward to examine pathogen dispersion, emphasizing bed proximity for effective infection control.

Airborne contaminants from a cubicle reaching the connecting corridor and other areas were below 20%. Ventilation in the corridor by exhaust from connected rooms was inefficient, and the airborne particle suspension paths were irregular and could remain suspended for over 5 min. Privacy curtains had a more significant effect on limiting particle dispersion than localized ventilation. Adopting both strategies was particularly effective. Lastly, spatial heterogeneity is critical in assessing the cross-infection risk in shared spaces.

This study characterizes long-range airborne transmission in large, shared hospital environments with submicron-sized aerosol trajectories under minimal external heat transfer. There is a need to consider submicron-sized aerosols in future studies for risk estimation as they exhibit long suspension time and irregular movement. Additionally, long-range airborne transmission concerning variations in air change rates should be explored to enhance infection control in inpatient wards and other healthcare settings.

Declaration of competing interest

None.

CRediT authorship contribution statement

Kwun Hei Cheung: Writing – original draft, Visualization, Validation, Software, Methodology, Investigation, Formal analysis, Data curation. **Tsz Wun Tsang:** Writing – review & editing, Supervision, Methodology, Conceptualization. **Kwok Wai Mui:** Writing – review & editing, Supervision, Project administration, Funding acquisition, Conceptualization. **Ling Tim Wong:** Writing – review & editing, Supervision, Methodology, Conceptualization.

Acknowledgments

This work was jointly supported by a grant from the Collaborative Research Fund (CRF) COVID-19 and Novel Infectious Disease (NID) Research Exercise and the General Research Fund, the Research Grants Council of the Hong Kong Special Administrative Region, China (project no. C5108-20G and Q86B), and PolyU Internal funding (project no. WZ2N, WZ3R, CE12, 1-52UD, and WZ9M).

Appendix

Table A1-A4 show the particle deposition results from the four simulation cases.

Table A1
Particle deposition in Case 1.

	Total	Infector		Patients from the same cubicle		Local exhausts		Curtain walls		Corridor		Washroom		Nursing station	
Bed location	Count	Count	%	Count	%	Count	%	Count	%	Count	%	Count	%	Count	%
A1	11025	6367	58	96	0.9	N/A		N/A		108	1.0	18	0.2	2	0.0
A2	10388	6586	63	79	0.8	N/A		N/A		134	1.3	11	0.1	2	0.0
A3	10094	4696	47	322	3.2	N/A		N/A		105	1.0	17	0.2	1	0.0
A4	10927	6401	59	305	2.8	N/A		N/A		59	0.5	7	0.1	2	0.0
A5	11074	6601	60	13	0.1	N/A		N/A		922	8.3	317	2.9	3	0.0
A6	10682	6650	62	50	0.5	N/A		N/A		512	4.8	23	0.2	36	0.3
B1	10878	7230	66	41	0.4	N/A		N/A		90	0.8	3	0.0	1	0.0
B2	11662	5462	47	139	1.2	N/A		N/A		435	3.7	9	0.1	3	0.0
B3	10927	5894	54	387	3.5	N/A		N/A		108	1.0	0	0.0	0	0.0
B4	10682	5439	51	162	1.5	N/A		N/A		164	1.5	2	0.0	0	0.0
B5	10780	7262	67	114	1.1	N/A		N/A		461	4.3	12	0.1	1	0.0
B6	11025	6220	56	26	0.2	N/A		N/A		1302	11.8	22	0.2	10	0.1
C1	10927	7699	70	45	0.4	N/A		N/A		124	1.1	0	0.0	3	0.0
C2	11074	7651	69	138	1.2	N/A		N/A		406	3.7	0	0.0	17	0.2
C3	10290	6030	59	283	2.8	N/A		N/A		123	1.2	0	0.0	7	0.1
C4	11319	5124	45	308	2.7	N/A		N/A		261	2.3	0	0.0	5	0.0
C5	10584	5853	55	38	0.4	N/A		N/A		1697	16.0	0	0.0	146	1.4
C6	9800	5282	54	62	0.6	N/A		N/A		675	6.9	0	0.0	0	0.0
D1	10290	6333	62	149	1.4	N/A		N/A		199	1.9	0	0.0	0	0.0
D2	11172	7515	67	29	0.3	N/A		N/A		73	0.7	0	0.0	0	0.0
D3	10731	6711	63	244	2.3	N/A		N/A		123	1.1	0	0.0	2	0.0
D4	9996	8040	80	163	1.6	N/A		N/A		91	0.9	0	0.0	1	0.0
D5	11074	7144	65	42	0.4	N/A		N/A		730	6.6	0	0.0	4	0.0
D6	11221	5976	53	48	0.4	N/A		N/A		1008	9.0	0	0.0	1	0.0

Table A2
Particle deposition in Case 2.

	Total	Infector		Patients from the same cubicle		Local exhausts		Curtain walls		Corridor		Washroom		Nursing station	
Bed location	Count	Count	%	Count	%	Count	%	Count	%	Count	%	Count	%	Count	%
A1	11025	5989	54	55	0.5	N/A		2005	18.2	126	1.1	2	0.0	0	0.0
A2	10388	5461	53	92	0.9	N/A		2101	20.2	79	0.8	1	0.0	1	0.0
A3	10094	6847	68	17	0.2	N/A		895	8.9	71	0.7	4	0.0	0	0.0
A4	10927	7227	66	17	0.2	N/A		1033	9.5	54	0.5	2	0.0	1	0.0
A5	11074	5793	52	14	0.1	N/A		1558	14.1	266	2.4	93	0.8	0	0.0
A6	10682	5203	49	18	0.2	N/A		2483	23.2	265	2.5	3	0.0	42	0.4
B1	10878	6390	59	48	0.4	N/A		1642	15.1	66	0.6	1	0.0	0	0.0
B2	11662	5840	50	120	1.0	N/A		1957	16.8	93	0.8	2	0.0	0	0.0
B3	10927	7723	71	16	0.1	N/A		1045	9.6	75	0.7	9	0.1	0	0.0
B4	10682	7098	66	12	0.1	N/A		960	9.0	51	0.5	3	0.0	0	0.0
B5	10780	3428	32	19	0.2	N/A		2507	23.3	377	3.5	101	0.9	0	0.0
B6	11025	4095	37	11	0.1	N/A		2033	18.4	419	3.8	1	0.0	5	0.0
C1	10927	4729	43	81	0.7	N/A		2205	20.2	124	1.1	0	0.0	3	0.0
C2	11074	7952	72	71	0.6	N/A		1049	9.5	81	0.7	0	0.0	1	0.0
C3	10290	7430	72	26	0.3	N/A		898	8.7	59	0.6	0	0.0	0	0.0
C4	11319	7005	62	30	0.3	N/A		875	7.7	72	0.6	0	0.0	0	0.0
C5	10584	4321	41	7	0.1	N/A		1925	18.2	359	3.4	0	0.0	88	0.8
C6	9800	3617	37	25	0.3	N/A		2778	28.3	412	4.2	0	0.0	1	0.0
D1	10290	5064	49	54	0.5	N/A		2033	19.8	137	1.3	0	0.0	1	0.0
D2	11172	5494	49	160	1.4	N/A		2254	20.2	104	0.9	0	0.0	0	0.0
D3	10731	7506	70	32	0.3	N/A		953	8.9	54	0.5	0	0.0	0	0.0
D4	9996	7342	73	18	0.2	N/A		1007	10.1	65	0.7	0	0.0	0	0.0
D5	11074	5172	47	14	0.1	N/A		1590	14.4	202	1.8	0	0.0	3	0.0
D6	11221	4069	36	5	0.0	N/A		2353	21.0	416	3.7	0	0.0	1	0.0

Table A3
Particle deposition in Case 3.

	Total	Infector		Patients from the same cubicle		Local exhausts		Curtain walls		Corridor		Washroom		Nursing station	
Bed location	Count	Count	%	Count	%	Count	%	Count	%	Count	%	Count	%	Count	%
A1	11025	4808	44	133	1.2	215	2.0	N/A		83	0.8	13	0.1	4	0.0
A2	10388	5826	56	64	0.6	41	0.4	N/A		107	1.0	8	0.1	12	0.1
A3	10094	6105	60	159	1.6	93	0.9	N/A		462	4.6	66	0.7	25	0.2
A4	10927	5974	55	56	0.5	973	8.9	N/A		279	2.6	16	0.1	31	0.3
A5	11074	4863	44	43	0.4	280	2.5	N/A		787	7.1	379	3.4	14	0.1
A6	10682	5326	50	22	0.2	326	3.1	N/A		917	8.6	12	0.1	546	5.1
B1	10878	5043	46	88	0.8	196	1.8	N/A		139	1.3	6	0.1	2	0.0
B2	11662	6856	59	43	0.4	779	6.7	N/A		59	0.5	3	0.0	2	0.0
B3	10927	7725	71	30	0.3	1322	12.1	N/A		58	0.5	4	0.0	0	0.0
B4	10682	7299	68	23	0.2	766	7.2	N/A		304	2.8	15	0.1	13	0.1
B5	10780	4740	44	57	0.5	401	3.7	N/A		602	5.6	285	2.6	12	0.1
B6	11025	5138	47	103	0.9	187	1.7	N/A		1269	11.5	14	0.1	144	1.3
C1	10927	5820	53	46	0.4	188	1.7	N/A		26	0.2	0	0.0	0	0.0
C2	11074	6207	56	56	0.5	632	5.7	N/A		40	0.4	0	0.0	1	0.0
C3	10290	6056	59	148	1.4	80	0.8	N/A		993	9.7	0	0.0	36	0.3
C4	11319	5879	52	91	0.8	1215	10.7	N/A		253	2.2	0	0.0	1	0.0
C5	10584	7099	67	55	0.5	207	2.0	N/A		367	3.5	0	0.0	12	0.1
C6	9800	4952	51	45	0.5	206	2.1	N/A		490	5.0	0	0.0	5	0.1
D1	10290	4421	43	68	0.7	75	0.7	N/A		52	0.5	0	0.0	0	0.0
D2	11172	5632	50	83	0.7	63	0.6	N/A		86	0.8	0	0.0	0	0.0
D3	10731	6275	58	93	0.9	218	2.0	N/A		303	2.8	0	0.0	0	0.0
D4	9996	5019	50	159	1.6	305	3.1	N/A		426	4.3	0	0.0	1	0.0
D5	11074	6352	57	9	0.1	1074	9.7	N/A		220	2.0	0	0.0	2	0.0
D6	11221	5150	46	9	0.1	591	5.3	N/A		679	6.1	0	0.0	0	0.0

Table A4
Particle deposition in Case 4.

	Total	Infector		Patients from the same cubicle		Local exhausts		Curtain walls		Corridor		Washroom		Nursing station	
Bed location	Count	Count	%	Count	%	Count	%	Count	%	Count	%	Count	%	Count	%
A1	11025	5812	53	3	0.0	162	1.5	670	6.1	45	0.4	2	0.0	0	0.0
A2	10388	5633	54	3	0.0	331	3.2	349	3.4	34	0.3	2	0.0	1	0.0
A3	10094	6876	68	3	0.0	434	4.3	617	6.1	40	0.4	1	0.0	0	0.0
A4	10927	6973	64	2	0.0	980	9.0	717	6.6	32	0.3	1	0.0	0	0.0
A5	11074	6553	59	5	0.0	175	1.6	1044	9.4	173	1.6	49	0.4	1	0.0
A6	10682	6044	57	2	0.0	255	2.4	1734	16.2	540	5.1	1	0.0	85	0.8
B1	10878	4954	46	2	0.0	433	4.0	829	7.6	89	0.8	5	0.0	3	0.0
B2	11662	6944	60	0	0.0	595	5.1	390	3.3	28	0.2	0	0.0	0	0.0
B3	10927	7495	69	1	0.0	797	7.3	886	8.1	24	0.2	3	0.0	1	0.0
B4	10682	6801	64	3	0.0	490	4.6	1008	9.4	41	0.4	2	0.0	2	0.0
B5	10780	6881	64	21	0.2	591	5.5	1337	12.4	161	1.5	49	0.5	0	0.0
B6	11025	7772	70	6	0.1	264	2.4	743	6.7	135	1.2	2	0.0	13	0.1
C1	10927	4783	44	4	0.0	225	2.1	874	8.0	32	0.3	0	0.0	0	0.0
C2	11074	4309	39	4	0.0	297	2.7	1533	13.8	39	0.4	0	0.0	0	0.0
C3	10290	7779	76	4	0.0	410	4.0	691	6.7	19	0.2	0	0.0	0	0.0
C4	11319	6885	61	3	0.0	109	1.0	836	7.4	62	0.5	0	0.0	2	0.0
C5	10584	6413	61	3	0.0	641	6.1	1132	10.7	197	1.9	0	0.0	12	0.1
C6	9800	5236	53	5	0.1	204	2.1	661	6.7	263	2.7	0	0.0	0	0.0
D1	10290	4905	48	3	0.0	706	6.9	373	3.6	15	0.1	0	0.0	1	0.0
D2	11172	4715	42	3	0.0	902	8.1	701	6.3	71	0.6	0	0.0	0	0.0
D3	10731	6607	62	2	0.0	1009	9.4	817	7.6	20	0.2	0	0.0	0	0.0
D4	9996	8241	82	0	0.0	424	4.2	737	7.4	28	0.3	0	0.0	0	0.0
D5	11074	4916	44	12	0.1	291	2.6	1707	15.4	231	2.1	0	0.0	3	0.0
D6	11221	7248	65	7	0.1	171	1.5	734	6.5	266	2.4	0	0.0	0	0.0

References

[1] S. Law, A.W. Leung, C. Xu, Severe acute respiratory syndrome (SARS) and coronavirus disease-2019 (COVID-19): from causes to preventions in Hong Kong, Int. J. Infect. Dis. 94 (2020) 156–163.
[2] A.A. Rabaan, S.H. Al-Ahmed, M.K. Al-Malkey, et al., Airborne transmission of SARS–CoV-2 is the dominant route of transmission: droplets and aerosols, Infez. Med. 29 (1) (2021) 10–19.
[3] W.K. Wang, S.Y. Chen, I.J. Liu, et al., Detection of SARS-associated Coronavirus in throat wash and saliva in early diagnosis, Emerg. Infect. Dis. 10 (7) (2004) 1213–1219.
[4] J.L. Santarpia, D.N. Rivera, V.L. Herrera, et al., Aerosol and surface contamination of SARS-CoV-2 observed in quarantine and isolation care, Sci. Rep. 10 (1) (2020) 13892.
[5] J. Jung, J. Lee, S. Jo, et al., Nosocomial outbreak of COVID-19 in a hematologic ward, J. Infect. Chemother. 53 (2) (2021) 332–341.
[6] V.C. Cheng, K.S. Fung, G.K. Siu, et al., Nosocomial outbreak of Coronavirus disease 2019 by possible airborne transmission leading to a superspreading event, Clin. Infect. Dis. 73 (6) (2021) e1356–e1364.
[7] X. Xie, Y. Li, A.T.Y. Chwang, et al., How far droplets can move in indoor environments–revisiting the Wells evaporation–falling curve, Indoor Air 17 (2007) 211–225.
[8] J.P. Duguid, The size and the duration of air-carriage of respiratory droplets and droplet-nuclei, J. Hyg. 44 (6) (1946) 471–479.
[9] N. Niazi, R. Groth, K. Spann, et al., The role of respiratory droplet physicochemistry in limiting and promoting the airborne transmission of human coronaviruses: a critical review, Environ. Pollut. 276 (2021) 115767.
[10] H. Ueki, Y. Furusawa, K. Iwatsuki-Horimoto, et al., Effectiveness of face masks in preventing airborne transmission of SARS-CoV-2, mSphere 5 (5) (2020) e00637 -20.
[11] G. La Rosa, M. Fratini, S.D. Libera, et al., Viral infections acquired indoors through airborne, droplet or contact transmission, Ann. Ist. Super. Sanita 49 (2) (2013) 124–132.
[12] World Health Organization (WHO), Roadmap to improve and ensure good indoor ventilation in the context of COVID-19, (2021), [Online]. Available: https://www.who.int/publications/i/item/9789240021280 [Accessed May 15, 2025].
[13] J. Liu, S. Zhu, M.K. Kim, et al., A review of CFD analysis methods for personalized ventilation (PV) in indoor built environments, Sustainability 11 (15) (2019) 4166.
[14] J. Zong, C. Lin, Z. Ai, Performance of low-volume air cleaner and local exhaust in mitigating airborne transmission in hospital outpatient rooms, Phys. Fluids 36 (1) (2024) 013342.
[15] H. Tan, M.H.D. Othman, H.Y. Kek, et al., Utilising localised exhaust and air curtain to reduce airborne particle settlement on surgical patients: potential future application in operating rooms? J. Therm. Anal. Calorim. 149 (2024) 11323–11336.
[16] J. Zhang, Y. Zhao, S. Wen, et al., Assessment of COVID-19 infection risk, thermal comfort, and energy efficiency in negative pressure isolation wards with varied ventilation modes, Energy Build. 308 (2024) 114002.
[17] L. Borro, L. Mazzei, M. Raponi, et al., The role of air conditioning in the diffusion of Sars-CoV-2 in indoor environments: a first computational fluid dynamic model, based on investigations performed at the Vatican State Children's hospital, Environ. Res. 193 (2021) 110343.
[18] M.K. Satheesan, K.W. Mui, L.T. Wong, A numerical study of ventilation strategies for infection risk mitigation in general inpatient wards, Build. Simul. 13 (2020) 887–896.
[19] J.H. Yang, FD analysis of the inhaled-air quality for the inpatients in a four-bed sickroom, J. Asian Archit. Build. Eng. 12 (1) (2013) 109–116.
[20] J. Gong, M. Chen, Numerical study of the influence of bedside curtains on human exhaled contaminants distribution in a two-bed ward, in: Proceedings of the E3S Web of Conferences, 356, 2022.
[21] J.H. Noh, J. Lee, K.C. Noh, et al., Effects of hospital ward curtains on ventilation in a four-bed hospital ward, Aerosol Air Qual. Res. 18 (2018) 2643–2653.
[22] C. Mendez, J.F. San Jose, J.M. Villafruela, et al., Optimization of a hospital room by means of CFD for more efficient ventilation, Energy Build. 40 (2008) 849–854.
[23] T.W. Tsang, L.T. Wong, K.W. Mui, et al., Preparing for the next pandemic: minimizing airborne transmission in general inpatient wards through management practices, Energy Build. 294 (2023) 113214.
[24] T.W. Tsang, K.W. Mui, L.T. Wong, Computational Fluid Dynamics (CFD) studies on airborne transmission in hospitals: a review on the research approaches and the challenges, J. Build. Eng. 63 (2023) 105533.
[25] G. Vita, D. Woolf, T. Avery-Hickmott, et al., A CFD-based framework to assess airborne infection risk in buildings, Build. Environ. 233 (2023) 110099.
[26] Y. Yang, H. Yang, Q. Li, et al., Simulation study on airflow organization and environment in reconstructed fangcang shelter hospital based on CFD, Buildings 13 (2023) 1269.
[27] Q. Zhou, H. Qian, L. Liu, Numerical investigation of airborne infection in naturally ventilated hospital wards with central-corridor type, Indoor Built Environ. 27 (1) (2018) 59–69.
[28] M. Jung, W.J. Chung, M. Sung, et al., Analysis of infection transmission routes through exhaled breath and cough particle dispersion in a general hospital, Int. J. Environ. Res. Public Health 19 (2022) 2512.
[29] L.T. Wong, H.C. Yu, K.W. Mui, et al., Drag constants for common indoor bioaerosols, Indoor Built Environ. 24 (3) (2015) 401–413.
[30] Y. Li, X. Huang, I.T.S. Yu, et al., Role of air distribution in SARS transmission during the largest nosocomial outbreak in Hong Kong, Indoor Air 15 (2004) 83–95.
[31] Z. Zhang, Q. Chen, Comparison of the Eulerian and Lagrangian methods for predicting particle transport in enclosed spaces, Atmos. Environ. 41 (2007) 5236–5248.
[32] B. Blocken, LES over RANS in building simulation for outdoor and indoor applications: a foregone conclusion? Build. Simul. 11 (2018) 821–870.
[33] Q. Chen, Comparison of different k-ε models for indoor airflow computations, Numer. Heat Transf. B Fundam. 28 (3) (1995) 353–369.
[34] R.K. Zeytounian, Joseph Boussinesq and his approximation: a contemporary view, C. R. Mec. 331 (2003) 575–586.
[35] J. Hang, Y. Li, R. Jin, The influence of human walking on the flow and airborne transmission in a six-bed isolation room: tracer gas simulation, Build. Environ. 77 (2014) 119–134.
[36] A.C.K. Lai, L.T. Wong, K.W. Mui, et al., An experimental study of bioaerosol (1-10 μm) deposition in a ventilated chamber, Build. Environ. 56 (2012) 118–126.

[37] L. Tian, Z. Lin, Q. Wang, et al., Numerical investigation of indoor aerosol particle dispersion under stratum ventilation and under displacement ventilation, Indoor Built Environ. 18 (4) (2009) 360–375.
[38] B. Zhao, Y. Zhang, X. Li, et al., Comparison of indoor aerosol particle concentration and deposition in different ventilated rooms by numerical method, Build. Environ. 39 (2004) 1–8.
[39] F. Li, J. Liu, J. Pei, et al., Experimental study of gaseous and particulate contaminants distribution in an aircraft cabin, Atmos. Environ. 85 (2014) 223–233.
[40] Y. Yan, X. Li, J. Tu, Effects of passenger thermal plume on the transport and distribution characteristics of airborne particles in an airliner cabin section, Sci. Technol. Built Environ. 22 (2016) 153–163.
[41] Z. Cao, K. Fang, X. Zhang, et al., Study on the sensitivity of steam ejector simulation to wall treatment methods, J. Phys. Conf. Ser. 2707 (2024) 012083.
[42] Y. Cheng, Z. Lin, Experimental investigation into the interaction between the human body and room airflow and its effect on thermal comfort under stratum ventilation, Indoor Air 26 (2016) 274–285.
[43] S. Kumar, M.D. King, Numerical investigation on indoor environment decontamination after sneezing, Environ. Res. 213 (2022) 113665.
[44] T. Lim, J. Cho, B.S. Kim, The influence of ward ventilation on hospital cross infection by varying the location of supply and exhaust air diffuser using CFD, J. Asian Archit. Build. Eng. 9 (1) (2010) 259–266.
[45] M.K. Satheesan, T.W. Tsang, K.W. Mui, et al., Optimal ventilation strategy for hospital inpatient wards, Paper presented at the Joint Symposium, (2023), Hong Kong, China.